Optics Letters

Watt-level widely tunable femtosecond mid-infrared $KTiOAsO_4$ optical parametric oscillator pumped by a 1.03 μm Yb:KGW laser

Xianghao Meng,[1,3] Zhaohua Wang,[1,*] Wenlong Tian,[2] Huijun He,[1,3] Shaobo Fang,[1] and Zhiyi Wei[1,3,4]

[1]Beijing National Laboratory for Condensed Matter Physics, Institute of Physics, Chinese Academy of Sciences, Beijing 100190, China
[2]School of Physics and Optoelectronic Engineering, Xidian University, Xi'an 710071, China
[3]University of Chinese Academy of Sciences, Beijing 100049, China
[4]e-mail: zywei@iphy.ac.cn
*Corresponding author: zhwang@iphy.ac.cn

Received 27 December 2017; revised 13 January 2018; accepted 15 January 2018; posted 19 January 2018 (Doc. ID 318524); published 15 February 2018

A high-power, high-repetition-rate, broadband tunable femtosecond optical parametric oscillator (OPO) is constructed based on $KTiOAsO_4$ crystal, pumped by a 75.5 MHz mode-locked Yb:KGW laser. With 7 W pump power, the OPO generates as much as 2.32 W of signal power at 1.55 μm and 1.31 W of idler power at 3.05 μm, corresponding to a total conversion efficiency of 51.8%. Operating at 151 MHz repetition rate, the wavelength of the signal covers 1.41–1.71 μm with a tunable idler range of 2.61–3.84 μm. The idler bandwidth is more than 180 nm over the entire mid-infrared range. By compensating intracavity dispersion, the signal pulse has a nearly Fourier transform-limited duration of 129 fs at 1.52 μm.

OCIS codes: (190.7110) Ultrafast nonlinear optics; (190.4970) Parametric oscillators and amplifiers; (190.4410) Nonlinear optics, parametric processes; (190.4400) Nonlinear optics, materials.

https://doi.org/10.1364/OL.43.000943

High-power, high-repetition-rate, continuously tunable femtosecond lasers in the near-infrared (NIR) and mid-infrared (MIR) ranges have many applications in various fields, such as time-resolved spectroscopy, optical microscopy, and pump-probe measurements [1–5]. Synchronously pumped femtosecond optical parametric oscillators (OPOs) based on nonlinear frequency conversion operating in the NIR region are potentially in great demand for optical communication to obtain optically high capacity and high data rates. The MIR femtosecond light sources are of particular importance in the research of a molecular "finger-print." Over the past decades, such femtosecond OPOs are typically pumped by Kerr-lens mode-locked Ti:sapphire oscillators [6–8]. Many nonlinear optical crystals such as $KTiOPO_4$ (KTP), $KTiOAsO_4$ (KTA), MgO-doped periodically poled lithium niobate (MgO:PPLN), periodically poled KTP (PPKTP), and periodically poled stoichiometric lithium tantalate (PPsLT) have been employed in the generation of femtosecond pulses through synchronously pumped OPOs. In 1997, Burr *et al.* reported a femtosecond OPO based on PPLN pumped by a Ti:sapphire oscillator at 793 nm, producing signals tunable over 1.12–1.5 μm with the maximum output power of 155 mW [7]. Several years later, Tillman *et al.* demonstrated a femtosecond OPO based on PPKTP pumped by a 76 MHz Ti:sapphire oscillator at 758 nm, generating a signal at 1.2 μm and an idler at 2.0 μm, and the maximum power conversion efficiency of the signal was 22% [9]. However, Ti:sapphire oscillator pumped OPOs typically generate average power of several hundred milliwatts limited by the available pump power, the low damage threshold, and the thin thickness of periodically poled nonlinear crystals. In addition, nonlinear optical crystals mentioned above exhibit large dispersion, which is disadvantageous for utilizing in femtosecond OPOs. Recently, ytterbium-doped fiber amplifiers and solid-state oscillators offer attractive properties for synchronously pumped femtosecond OPOs, such as high power, good beam quality, and low cost compared to Ti:sapphire oscillators [10–14]. Previously, Cleff *et al.* demonstrated a femtosecond OPO based on LiB_3O_5 (LBO) pumped by a frequency-doubled Yb-fiber amplifier, providing tunable idler pulses between 1.19 and 1.63 μm with a maximum power of 300 mW [15]. In 2011, Hegenbarth *et al.* reported a femtosecond OPO based on MgO:PPLN crystal pumped by a 7.4 W femtosecond Yb: KGW laser [16]. In 2016, we reported a high-power femtosecond OPO based on BiB_3O_6 (BIBO) crystal, widely tunable from the visible to NIR band [17]. Among the nonlinear crystals, the KTA combines the high optical damage threshold (>1.2 GW/cm^2) [18] and the high effective nonlinear coefficient (deff ~ 3 pm/V). The optical transmission wavelength of KTA extends to $\lambda \sim 5.3$ μm in the MIR range, much wider than that of 3 μm in the BIBO and LBO. Although the effective nonlinear coefficient of KTA is lower than PPLN, KTA has great advantages in high-power near-1-μm-pumped

femtosecond OPOs owing to its higher optical damage threshold and lower group velocity dispersion (GVD).

In this Letter, we report a high-power, high-repetition-rate broadband tunable femtosecond KTA OPO pumped by a femtosecond mode-locked Yb:KGW laser. Using a 2-mm-long KTA, the tunable signal wave within the wavelength range from 1.41 to 1.71 μm has been produced, with a tunable idler range of 2.61–3.84 μm operating at 151 MHz by varying the phase-matching angle and optimizing the cavity length. With 7 W pump power, the OPO is able to simultaneously support as high as 2.32 W of signal power at 1.55 μm and 1.31 W of MIR idler power at 3.05 μm, corresponding to a total conversion efficiency of 51.8%. The pulse width of the signal wave is measured to be 129 fs at 1.52 μm close to the transform-limited pulse duration. In addition, the signal and idler powers have fluctuations of less than 2% RMS over 1 h.

The experimental configuration of the KTA OPO system for tunable femtosecond MIR pulses is shown in Fig. 1. The pump source is a commercial femtosecond Kerr-lens mode-locked Yb:KGW laser (Light Conversion, Flint6.0) with up to 7 W average power at 1.03 μm. Operating at 75.5 MHz repetition rate, the pump laser produces 100 fs pulses with 10.1 nm spectral bandwidth. The output beam from the pump laser has a quality factor of $M^2 \sim 1.2$ and diameter of 1.4 mm. A half-wave plate (HWP1) and a polarizing beam splitter (PBS) are employed as a variable attenuator to change the power of the pump pulses. A second half-wave plate (HWP2) is used to adjust the polarization for the optimal phase-matching direction in the KTA crystal. The pump pulses are focused into the KTA crystal by a lens (L1) with 100 mm focal length, corresponding to a beam waist of 44 μm at the focus. The signal single resonant OPO has a linear standing-wave cavity comprising two concave mirrors, C1 and C2 (100 mm ROC), three high reflection mirrors (HR1, HR2 and HR3), and a 1% plane output coupler (OC). All mirrors are deliberately coated to support high transmission at 1.03 μm for the pump and high reflection for the signal in the range of 1.23–1.72 μm. In addition, C2 provides high transmission ($T > 95\%$) for the idler at 2.2–4.4 μm. The KTA crystal is cut at $\theta = 41.3°$, $\varphi = 0°$ for type-II phase matching in the xz-plane ($o \rightarrow e + o$) with a length of 2 mm, coated with high transmission at both 1.03 μm and 1.3–1.75 nm. A germanium filter lens (L_2, $f = 100$ mm) is used as the dichroic mirror to separate and collimate the generated idler from the residual pump that is a high reflection coating ($R > 95\%$) over 3–5 μm. The total cavity length of the OPO is set to 993 mm corresponding to a repetition rate of 151 MHz, which is twice that of the Yb:KGW oscillator.

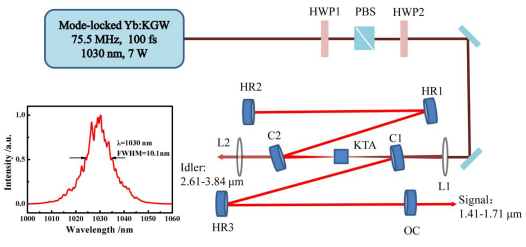

Fig. 1. Schematic of the experimental setup for KTA femtosecond OPO. L1, L2, lenses; HWP1, HWP2, half-wave plates; PBS, polarizing beam splitter; C1, C2, concave spherical mirrors; HR1, HR2, plane mirrors; OC, 1% output coupler. Inset: spectrum of the pump pulse.

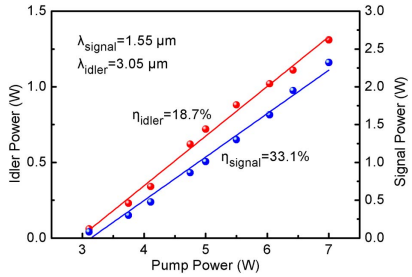

Fig. 2. Variation of the signal (1.55 μm) and idler (3.05 μm) output powers extracted from the KTA OPO as a function of the pump power.

The stable output of the signal wave is achieved when the cavity length of the KTA OPO system is accurately matched to half of that of the Yb:KGW laser. Figure 2 presents the variation of signal and idler output power as a function of the pump power. The signal and idler powers increase linearly up to the maximum pump power. With 7 W pump power, the OPO produces 2.32 W signal pulses at 1.55 μm and 1.31 W idler pulses at 3.05 μm, respectively. It corresponds to 33.1% pump-to-signal power conversion and 18.7% pump-to-idler power conversion. The total power conversion efficiency adds up to 51.8%. Although the pump laser has a high spatial beam quality and a high peak power, the pump threshold of the OPO is as high as 3.11 W. It can be explained that the short output pulse has a large bandwidth so that a high pump power is required to make all components in such a broad band exceed the threshold together. By varying the phase-matching angle of KTA and optimizing the cavity length, the wavelength of the signal wave can be tuned from 1.41 to 1.71 μm together and the idler from 2.61 to 3.84 μm. The cavity length tuning is mainly governed by the dispersion of the nonlinear materials. Only the signal wave in resonance with the pump cavity length can achieve gain effectively because the group velocity is different for different signal wavelengths. Figure 3 illustrates the wavelength dependence of the signal power and the idler power as the pump is fixed at 7 W. The average power of the signal pulse in the entire tuning range (1.41–1.71 μm) exceeds 450 mW while the idler power varies from a maximum of 1.31 W at 3.05 μm–90 mW at 2.61 μm. The idler power exceeds 400 mW over 70% of the tuning range (2.8–3.5 μm).

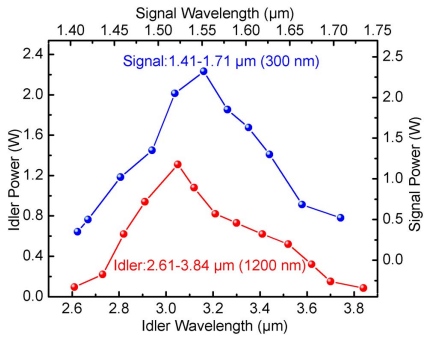

Fig. 3. Extracted signal and idler output powers across the tuning range of the KTA OPO at a fixed pump power.

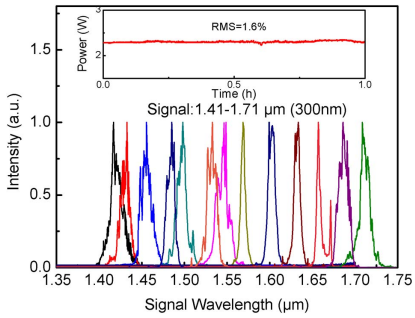

Fig. 4. Normalized signal spectra across the tuning range of the femtosecond KTA OPO. Inset: long-term power stability for 1 h at the central wavelength of 1.55 μm.

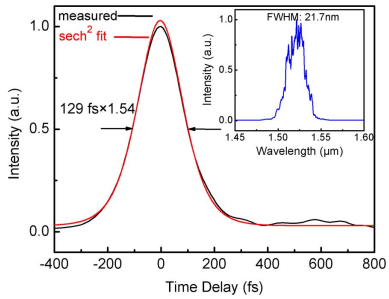

Fig. 5. Typical intensity autocorrelation trace of the OPO signal pulses at 1.52 μm with a duration of 129 fs (×1.543, assuming a sech^2 pulse shape). Inset: the corresponding optical spectrum.

Although the spectral transmittance of KTA extends from 350 nm in the UV up to 5.3 μm in the MIR range, the idler power decreases toward longer wavelengths because KTA has intense absorption in the range of 3.5–5.3 μm, resulting in low transmission. The decrease in the short wavelength below 3 μm is caused by the low transmittance of the germanium filter, supporting transmission across 3–5 μm.

Figure 4 displays the normalized output signal spectra in the tuning range of the KTA OPO. By varying the angle of KTA and the cavity length, the OPO supports signal pulses tunable from 1.41–1.71 μm measured by an optical spectrum analyzer (Yokogawa, AQ6370C). The KTA OPO can withstand about 20 μm cavity length variation, resulting in a signal wavelength shift of almost 60 nm before the signal wave disappears. The cavity roundtrip time of signal pulses depends on the wavelength through the contribution of the group velocity inside the KTA crystal. It is noticed that the shortest wavelength of the signal is close to 1.41 μm limited by the phase-matching condition of the KTA crystal pumped at the central wavelength of 1.03 μm. The longest wavelength extends to 1.71 μm limited by the coating on the concave and plane mirrors (high reflection across 1.23–1.72 μm). To demonstrate the long-term stability of the signal pulse, we measure the output power at a wavelength of 1.55 μm while stabilizing the cavity length. As shown in the inset of Fig. 4, the noise RMS is 1.6% over 1 h at the maximum output power of 2.32 W. The instability is due to the disturbance of the environment, such as air turbulence and mechanical vibration.

The group velocity dispersion (GDD) induced by the elements in the cavity can be calculated according to the second-order derivative of refraction equation. In a 2-mm-long KTA crystal, the average GDD is 128 fs^2 between the signals from 1.41 to 1.71 μm and the pump of 1.03 μm. The GDD induced by air with a length of 0.994 m is close to 20 fs^2 for the laser at the central wavelength of 1.52 μm. To obtain a near Fourier-transform-limited pulse duration from the KTA OPO, a pair of concave chirped mirrors (C1 and C2) with −100 fs^2 GDD (coating at 1.44–1.72 μm) for each piece are used to compensate the positive intracavity dispersion introduced by the KTA crystal and air. Figure 5 shows a typical intensity autocorrelation trace at a signal wavelength of 1.52 μm, where the signal output power is 1.51 W for 7 W pump power. The pulse duration at FWHM is measured as 129 fs by an autocorrelator (PulseCheck-50, A. P. E. GmbH), assuming a sech^2 pulse shape. As shown in the inset of Fig. 5, the signal spectrum is centered at 1.52 μm with a FWHM spectral bandwidth of 21.7 nm, and the corresponding Fourier-transform-limited pulse duration is 114 fs, calculated by Fourier transforming the spectrum without dispersion. These two measurements deliver a $\Delta\tau\Delta\nu = 0.36$, confirming a near-transform-limited pulse. Across the NIR tuning range, signal pulse durations in the range of 129–200 fs are measured, with the time-bandwidth products changing from 0.36 to 0.6. The pulse broadening is due to the group velocity mismatch (GVM) between the interacting waves in the crystal.

The MIR idler performance is characterized behind L2. The spectrum of the MIR idler is measured by a monochromator (Omni-λ 150, Zolix Instruments Ltd.) combined with an HgCdTeZn infrared detector (Vigo System), an optical chopper, and a phase-locked loop amplifier (SR830 Stanford Research Systems). The modulation frequency of the chopper and amplifier is set to 100 Hz. Figure 6 shows the typical normalized spectra of the idler pulses extracted from the KTA OPO. The central wavelength of the idler is tunable from 2.61 to 3.84 μm. The corresponding FWHM bandwidths of the idler are more than 180 nm over the entire tuning range with a maximum of 340 nm at the central wavelength of 3.41 μm. It is noted that some modulations appear in the idler spectra although the idler pulses are single passing the KTA crystal; this can be attributed to the atmospheric absorption. The OPO setup is located in a dry environment, while the idler pulses have to travel a distance of about 0.8 m outside the monochromator. In addition, the MIR idler output power is recorded to be stable with a fluctuation of less than 1.5% rms within 1 h. This illustrates that single-step nonlinear

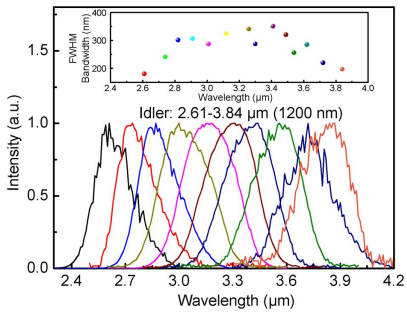

Fig. 6. Typical normalized idler spectra across the KTA OPO tuning range. Inset: the corresponding FWHMs of the idler spectra as a function of the wavelength.

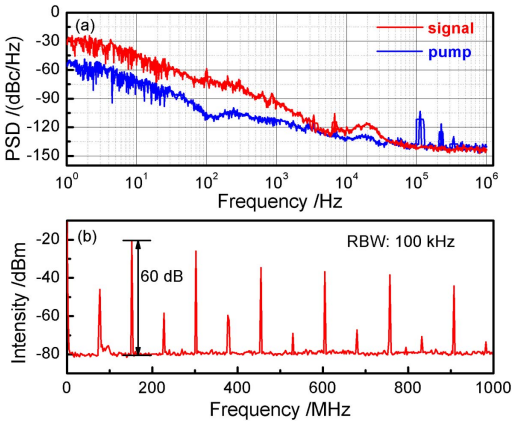

Fig. 7. (a) Phase noise PSD of signal (red) and pump (blue) from 1 Hz to 1 MHz; (b) typical radio-frequency spectrum from 0 Hz to 1 GHz with 100 KHz resolution.

conversion for MIR generation has advantages in terms of long-term stability compared to cascaded nonlinear optical processes.

The signal pulse train is detected by a commercial spectrum analyzer (R&S FSW26). Figure 7(a) depicts the phase noise power spectral density (PSD) of signal and pump from 1 Hz to 1 MHz. When the signal operates at the central wavelength of 1.55 μm with the maximum output power, the measure PSD of the signal exhibits slightly higher noise in the range of 1 Hz ~ 5 kHz compared to the Yb:KGW pump laser. The higher phase noise may be caused by the disturbance of the environment. Both the OPO signal and Yb:KGW oscillator present low noise with shot-noise-limited performance (−143 dB/Hz) from 100 kHz onward. The low noise level of the OPO signal in the entire range is attributed to the all-solid-state pump laser. The typical radio-frequency (RF) spectrum of the output signal pulses is measured by an RF spectrum analyzer (Agilent E4402B). Figure 7(b) is the wide spectrum measurement that shows the high harmonics of the fundamental frequency, spanning 1 GHz with a resolution of 100 kHz. It is noticed that the fundamental beat note at 151 MHz reveals a high signal-to-noise ratio of 60 dB from the central spike. The clean RF spectrum indicates the OPO signals at 151 MHz synchronize well to the second harmonic of the pump laser repetition rate of 75.5 MHz. Except for the 151 MHz repetition frequency, the other harmonic frequencies also exist owing to the periodic modulation of the signals at the repetition rate of 75.5 MHz, which is equal to the that of the pump laser.

In conclusion, we have demonstrated a high-power, high-repetition-rate femtosecond OPO based on KTA crystal pumped by a Kerr-lens mode-locked Yb:KGW laser. The signal wavelength is tunable from 1.41 to 1.71 μm together with idler tuning from 2.61 to 3.84 μm at 151 MHz by varying the phase-matching angle of KTA and the cavity length. The FWHM bandwidth of the idler is more than 180 nm across the entire MIR tuning range, with a maximum of 340 nm at a central wavelength of 3.41 μm. By using a 1% OC, the OPO simultaneously provides as high as 2.32 W of signal power at 1.55 μm and 1.31 W of MIR idler power at 3.05 μm, corresponding to a total conversion efficiency of 51.8%. The signal pulse extracted from the intracavity dispersion-compensated KTA OPO has a nearly transform-limited pulse duration of 129 fs at 1.52 μm. The power fluctuation of signal and idler is less than 2% RMS over 1 h. We not only obtain the widely tunable MIR range from 2.61 to 3.84 μm but also realize the watt-level output power. Such a high-power broadband tunable NIR and MIR femtosecond source is potentially of great interest for ultrafast spectroscopy and frequency comb generation.

Funding. Strategic Priority Research Program of Chinese Academy of Sciences (XDB16030200); Key Research Program of Frontier Sciences of Chinese Academy of Sciences (KJZD-EW-L11-03); National Key Scientific Instruments Development Program of China (2012YQ120047); National Natural Science Foundation of China (NSFC) (11774410, 61575217, 61575219); National Key R&D Program of China (2017YFC0110301).

Acknowledgment. We thank Professor Guoqing Chang, Kun Zhao, and Quanli Dong for useful discussion and manuscript revision. We thank the funding supported by the National Key Scientific Instruments Development Program of China, the National Natural Science Foundation of China, the Strategic Priority Research Program of Chinese Academy of Sciences, the National Key R&D Program of China, and the Key Research Program of Frontier Sciences of Chinese Academy of Sciences.

REFERENCES

1. G. M. Gale, G. Gallot, F. Hache, N. Lascoux, S. Bratos, and J.-C. Leicknam, Phys. Rev. Lett. **82**, 1068 (1999).
2. M. Drescher, M. Hentschel, R. Kienberger, M. Uiberacker, V. Yakovlev, A. Scrinzi, T. Westerwalbesloh, U. Kleineberg, U. Heinzmann, and F. Krausz, Nature **419**, 803 (2002).
3. J. M. Ingram and A. W. Fountain III, Appl. Spectrosc. **61**, 1254 (2007).
4. A. Assion, M. Geisler, J. Helbing, V. Seyfried, and T. Baumert, Phys. Rev. A **54**, R4605 (1996).
5. J. G. Fujimoto, J. M. Liu, E. P. Ippen, and N. Bloembergen, Phys. Rev. Lett. **53**, 1837 (1984).
6. D. C. Edesltein, E. S. Wachman, and C. L. Tang, Appl. Phys. Lett. **54**, 1728 (1989).
7. K. C. Burr, C. L. Tang, M. A. Arbore, and M. M. Fejer, Appl. Phys. Lett. **70**, 3341 (1997).
8. A. E. Martin, O. Kokabee, and M. E. Zadeh, Opt. Lett. **33**, 2650 (2008).
9. K. A. Tillman, D. T. Reid, D. Artigas, J. Hellström, V. Pasiskevicius, and F. Laurell, J. Opt. Soc. Am. B **20**, 1309 (2003).
10. C. Gu, M. Hu, J. Fan, Y. Song, B. Liu, and C. Wang, Opt. Lett. **39**, 3896 (2014).
11. S. C. Kumar, J. Krauth, A. Steinmann, K. T. Zawilski, P. G. Schunemann, H. Giessen, and M. E. Zadeh, Opt. Lett. **40**, 1398 (2015).
12. Z. Zhang, D. T. Reid, C. Kumar, M. E. Zadeh, P. G. Schunemann, K. T. Zawilski, and C. R. Howle, Opt. Lett. **38**, 5110 (2013).
13. T. Steinle, F. Mörz, A. Steinmann, and H. Giessen, Opt. Lett. **41**, 4863 (2016).
14. R. Hegenbarth, A. Steinmann, S. Sarkisov, and H. Giessen, Opt. Lett. **37**, 3513 (2012).
15. C. Cleff, J. Epping, P. Gross, and C. Fallnich, Appl. Phys. B **103**, 795 (2011).
16. R. Hegenbarth, A. Steinmann, J. Hebling, and H. Giessen, J. Opt. Soc. Am. B **28**, 1344 (2011).
17. W. Tian, Z. Wang, X. Meng, N. Zhang, J. Zhu, and Z. Wei, Opt. Lett. **41**, 4851 (2016).
18. W. R. Bosenberg, L. K. Cheng, and J. D. Bierlein, Appl. Phys. Lett. **65**, 2765 (1994).